RESEARCH ARTICLE | FEBRUARY 05 2019

Hierarchical multi-mode molecular stress function (HMMSF) model for linear and LCB polymer melts FREE

Esmaeil Narimissa ✉; Manfred H. Wagner

AIP Conf. Proc. 2065, 030043 (2019)
https://doi.org/10.1063/1.5088301

Hierarchical Multi-Mode Molecular Stress Function (HMMSF) Model for Linear and LCB Polymer Melts

Esmaeil Narimissa[a] and Manfred H. Wagner[b]

[a] *Deptartment of Chemical Engineering, Guangdong Technion–Israel Institute of Technology (GTIIT), Shantou 515063, China*

[b] *Polymer Engineering/Polymer Physics, Berlin Institute of Technology (TU Berlin), Fasanenstrasse 90, 10623 Berlin, Germany*

[a] Corresponding author: esmaeil.narimissa@gtiit.edu.cn

Abstract. We [1-6] have developed a novel Hierarchical Multi-mode Molecular Stress Function (HMMSF) model for linear and long-chain branched (LCB) polymer melts implementing the basic ideas of (i) hierarchical relaxation, (ii) dynamic dilution, (iii) interchain tube pressure, and (iv) convective constraint release. The excellent predictions of this model were demonstrated in uniaxial, equibiaxial, and planar extensional deformation for linear and LCB melts, as well as in shear flow for a LCB polymer, with a minimum number of adjustable free nonlinear material parameters, i.e. one in the case of extensional flows, and two in shear flow.

Keywords: Rheological Modeling, Extensional Flow, Shear Flow, Polymer Melt, Molecular Stress Function
PACS: 83.10.Gr, 83.50.Jf, 83.60.Df, 83.80.Sg

INTRODUCTION

The significance of the extensional rheological analysis of polymer melts is resulted from the subjection of nearly all polymer processing systems to extensional deformation at narrowing profile sections, where extensional flow dominates the rheological characteristics of the deformation [7-10]. This dominance is accentuated in processes such as blow moulding, melt spinning, and biaxial stretching of extruded sheets, and the extensional deformation may be the last step before solidification which triggers molecular orientation [11, 12]. The occurrence of strain hardening behaviour prevents the formation of local weak spots as the starting point of cracks in plastic melts in free surface flows. Moreover, extensional deformations are very sensitive to macromolecular structure of the polymeric systems including degree of branching, molecular weight distribution, and cross-linking [12, 13]. Both linear and branched polymers exhibit strain hardening. Strain hardening is markedly affected by the architecture of the polymers when the existence and abundance of branches as well as the number of the entanglements of the backbone directly impacts the strength and the onset of this rheological phenomenon.

The importance of the relationship between the molecular structure and rheological behaviour of polymeric systems is due to the considerable sensitivity of the rheological properties to the structural ones, as well as the principal role of the rheological characteristics in flow behaviour during the melt processing of the polymers [14]. The recent developments of quantitative mathematical models to analyse molecular structures through rheological properties has led to the evolution of the molecular structural aspects through rheological measurements, and vice versa, the prediction of the rheological aspects when the molecular structure is understood. The integration of the rheological modelling into the polymerization reactions and melt forming operations can result in the prediction of the detailed molecular structure of polymers, prediction of the rheological properties based on the structure, and the prediction of the detailed processing behaviour of polymers via numerical flow simulation techniques based on quantified rheological parameters [14]. Therefore, the significance of the rheological modelling of polymeric systems has encouraged us to develop a comprehensive constitutive model [1-5] capable of the prediction of rheological behaviours of Long-Chain Branched (LCB) and linear polymers for different categories of flow, i.e. uniaxial extensional, multiaxial extensional, and shear deformations with minimum number of free parameters (i.e. one in extensional and two in shear flows).

Proceedings of PPS-34
AIP Conf. Proc. 2065, 030043-1–030043-5; https://doi.org/10.1063/1.5088301
Published by AIP Publishing. 978-0-7354-1793-9/$30.00

THEORETICAL BACKGROUND

The detailed theoretical steps behind the development of the Hierarchical Multi-Mode Molecular Stress Function (HMMSF) Model were presented in [1-4] for uniaxial and multiaxial extensional flow, and in [5] for shear flow of polymer melts. Here, we present a reduced number of well-defined and extremely simple set of constitutive relations comprising the rheology of both linear and LCB melts.

The extra stress tensor of the Hierarchical Multi-mode MSF (HMMSF) model [1] is given as,

$$\sigma(t) = \sum_i \int_{-\infty}^{+\infty} \frac{\partial G_i(t-t')}{\partial t'} f_i^2(t,t') \mathbf{S}_{DE}^{IA}(t,t') dt' \tag{1}$$

Here $\mathbf{S}_{DE}^{IA}$ is the Doi and Edwards orientation tensor assuming an independent alignment (IA) of tube segments [15], which is five times the second order orientation tensor **S**,

$$\mathbf{S}_{DE}^{IA}(t,t') \equiv 5\left\langle \frac{\mathbf{u}'\mathbf{u}'}{\mathrm{u}'^2} \right\rangle = 5\mathbf{S}(t,t') \tag{2}$$

u´ presents the length of the deformed unit vector **u´**, and the bracket denotes an average over an isotropic distribution of unit vectors at time t´, **u**(t´), which can be expressed as a surface integral over the unit sphere. The molecular stress functions $f_i = f_i(t,t')$ are the inverse of the relative tube diameters a_i of each mode *i*,

$$f_i(t,t') = a_{i0} / a_i(t,t') \tag{3}$$

$f_i = f_i(t,t')$ is a function of both the observation time *t* and the time of creation of tube segments by reptation *t'*. The relaxation modulus *G(t)* of the melt is represented by discrete Maxwell modes with partial relaxation moduli g_i and relaxation times τ_i,

$$G(t) = \sum_{j=1}^{n} G_i(t) = \sum_{j=1}^{n} g_j \exp(-t/\tau_j) \tag{4}$$

The mass fraction w_i of dynamically diluted linear or LCB polymer segments with relaxation time $\tau_i > \tau_D$ is determined by considering the ratio of the relaxation modulus at time $t = \tau_i$ to the dilution modulus $G_D = G(t = \tau_D)$,

$$\begin{aligned} w_i^2 &= \frac{G(t=\tau_i)}{G_D} = \frac{1}{G_D}\sum_{j=1}^{n} g_j \exp(-\tau_i/\tau_j) \quad \text{for } \tau_i > \tau_D \\ w_i^2 &= 1 \qquad\qquad\qquad\qquad\qquad\qquad\quad \text{for } \tau_i \le \tau_D \end{aligned} \tag{5}$$

It is assumed that the value of w_i obtained at $t = \tau_i$ can be attributed to the chain segments with relaxation time τ_i. Segments with $\tau_i < \tau_D$ are considered to be permanently diluted, i.e. their weight fractions are fixed at $w_i = 1$. Although this may seem to be a very rough estimate, it was shown to be a sufficiently robust assumption to model the rheology of broadly distributed polymers, largely independent of the number of discrete Maxwell modes used to represent the relaxation modulus *G(t)* [1]. The evolution equation for the molecular stress function of each mode is expressed as [1],

$$\frac{\partial f_i}{\partial t} = f_i(\mathbf{K}:\mathbf{S}) - \frac{1}{\alpha}\left(\frac{1}{\tau_i} + \beta CR\right)\left[(f_i - 1)\left(1 - \frac{2}{3}w_i^2\right) + \frac{2}{9}f_i^2(f_i^3 - 1)w_i^2\right] \tag{6}$$

with the initial conditions $f_i(t = t', t) = 1$. The first term on the right hand side represents an on average affine stretch rate with **K** the velocity gradient tensor, the second term takes into account Rouse relaxation in the longitudinal direction of the tube, and the third term limits molecular stretch due to the interchain tube pressure in the lateral direction of a tube segment [16]. The topological parameter α depends on the topology of the melt, with

$$\begin{aligned} \alpha &= 1 \qquad \text{for LCB Melts} \\ \alpha &= 1/3 \qquad \text{for polydisperse linear melts} \end{aligned} \tag{7}$$

CR represents a dissipative Constraint Release (CR) term in shear flow (zero in extensional flow) relating the linear-viscoelastic relaxation times τ_i by constraint release relaxation times τ_{iCR} defined as [5, 17],

$$\frac{1}{\tau_{iCR}} = \frac{1}{\tau_i} + \beta\, CR \tag{8}$$

β is the numerical coefficient of the CCR mechanism considered as a fitting parameter.

COMPARISON BETWEEN HMMSF MODEL PREDICTIONS WITH EXPERIMENTAL DATA

In this section, we present the application of the HMMSF model (Eqs. (1), (5), (6), and (7)) for the prediction of the extensional and shear rheological behaviours of LCB and linear melts. The modelling was performed on well-characterized Low-Density Polyethylene (LDPE I), and High-Density Polyethylene (HDPE I) data of Hachmann [18] and Hachmann and Meissner [19]; and Bastian [20], respectively. The characterization of the polymers (i.e. weight average molecular weight (M_w), number average molecular weight (M_n), polydispersity index (M_w/M_n), melting temperature (T_m), room temperature density (ρ_{RT}), testing temperature density (ρ_T), zero shear viscosity at testing temperature (η_0), melt flow index (MFI), activation energy (E_a), dilution modulus G_D obtained by fitting of the extensional data, and the linear-viscoelastic relaxation spectrum) can be found in [2, 3, 5].

The symbols in **Fig. 1** present the uniaxial, equibiaxial, and planar transient viscosities (μ_u, μ_e, μ_{p1}, and μ_{p2}, respectively) of LDPE at 150°C. The predictions of the HMMSF model are illustrated using continuous lines in this figure. The HMMSF model shows a very good agreement with the uniaxial extensional viscosity of LDPE during the strain hardening regime and its transition to the steady-state extensional viscosity (**Fig.1a**). **Figure 1b** shows that the predictions of the HMMSF model are in excellent quantitative agreement with the equibiaxial viscosity of LDPE. Moreover, our model presents a remarkably well prediction of planar extensional viscosity of LDPE in the direction of flow (η^+_{P1}), and cross viscosity (η^+_{P2})of the planar extensional mode in both qualitative and quantitative scales (**Fig. 1c,** and **1d**).

The HMMSF model demonstrates excellent agreement with the uniaxial extensional viscosity of HDPE I (**Fig. 2a**) in the strain hardening regime and, as far as accessible by the experiments, in the transition to what seems to be the steady-state elongational viscosity. **Figure 2b** show that the predictions of the HMMSF model are also in very good agreement with the equibiaxial viscosity data of HDPE I. Likewise, the model presents a remarkably fine prediction of the planar extensional viscosities of HDPE I in the direction of flow as well as in the cross-flow direction (η^+_{P1} and η^+_{P2}) (**Figs. 2c** and **2d**, respectively).

Figure 3 displays the comparison between the predictions of the HMMSF model with a CR term and the shear data. Constraint release parameters $\beta=0.14$ (for LDPE I in **Figs. 3a**, and **3b**), and $\beta=1$ (for HDPE I in **Figs. 3c**, and **3d)** lead to good agreement of predictions with the shear data for both low and high shear rate deformations. The prediction of the maxima of the first normal stress function are in good accordance with the observed maxima particularly at high shear rates (**Fig. 3b**, and **3d**). However, the incidence of the experimental delay of the rise-time prevents a direct comparison between our model and the data. Nevertheless, we can shift the predictions of the model at high shear rates in time to mimic the experimental delays of the instrument, as shown in [5].

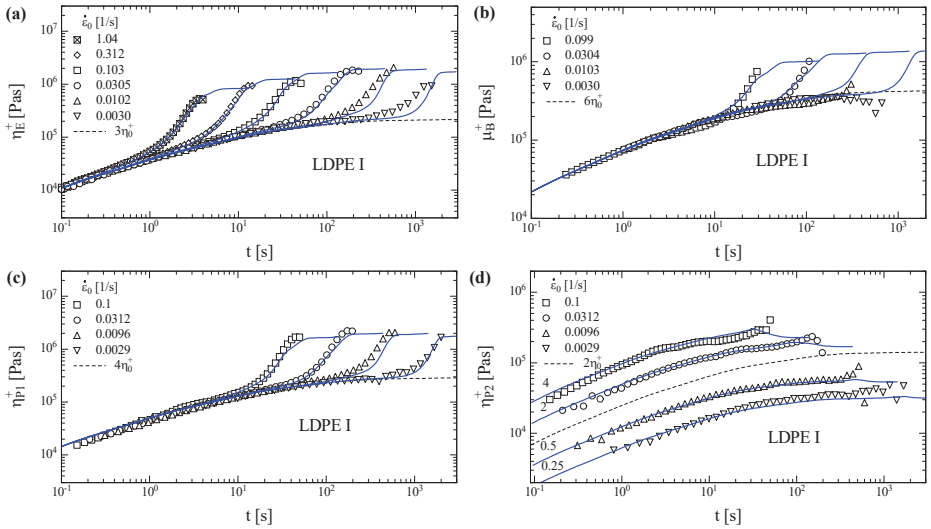

FIGURE 1. Comparison of (a) uniaxial, (b) equibiaxial, as well as (c and d) first and second planar viscosity data (symbols) of LDPE I (Lupolen 1810H) melt at 150ºC with predictions of the HMMSF model (Eqs. (1), (5), (6), and (7), continuous lines) for a dilution modulus of G_D=*1.5E+4Pa*. Dotted line indicates the linear-viscoelastic start-up viscosities. Data and lines in (d) are shifted by factors 4, 2, 0.5 and 0.25 vertically. Reprinted by permission from Springer[2] Copyright (2016).

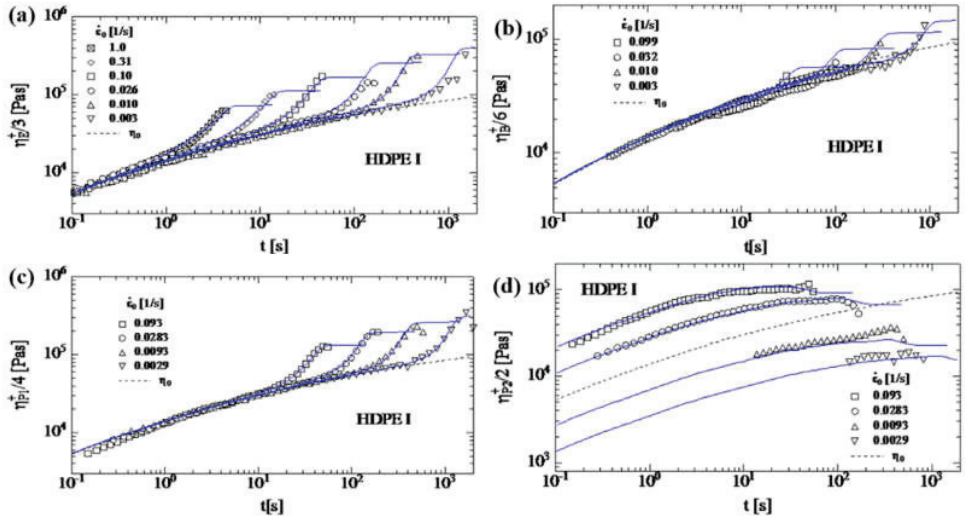

FIGURE 2. Modelling of (a) uniaxial, (b) equibiaxial, (c) first planar, and (d) second planar extensional viscosity data (symbols) of HDPE I by the HMMSF model (Eqs. Eqs. (1), (5), (6), and (7), continuous lines) at 150 °C with dilution modulus G_D=8.0E+2 Pa. Dotted line indicates linear-viscoelastic start-up viscosities. Reprinted with permission from AIP Publishing[3]. Copyright [2016], The Society of Rheology.

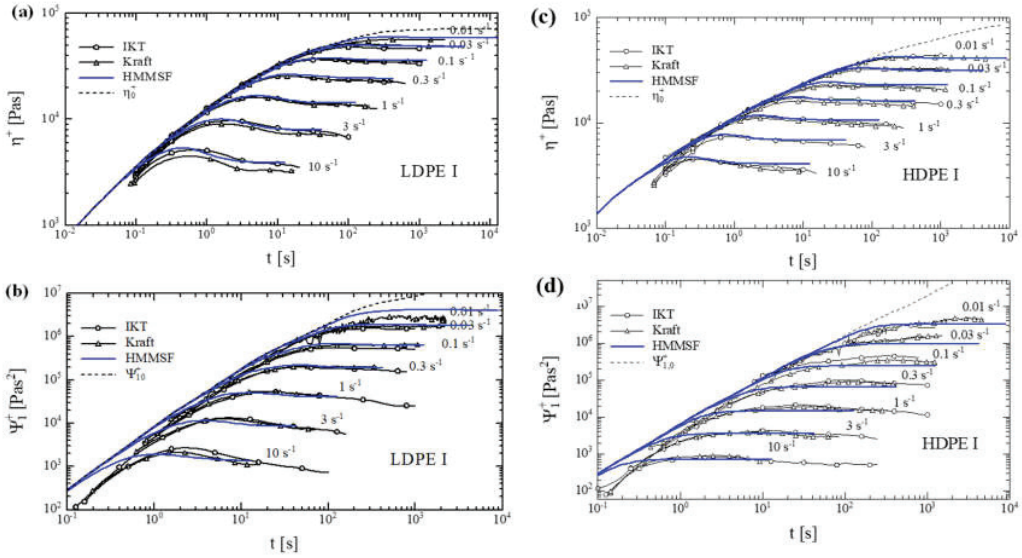

FIGURE 3. Comparison of the predictions (blue lines) of the HMMSF model including the CR term (Eqs. Eqs. (1), (5), (6), and (7)) with G_D=*1.5E+4Pa* and β=*0.14* for LDPE I at 150 °C with (a) shear viscosity and (b) first normal stress function data (lines with symbols); and with G_D=*800 Pa* and β=*1* for HDPE I at 170 °C with (a) shear viscosity and (b) first normal stress function data (lines with symbols). Data by Kraft [21] and Bastian [20, 22] (IKT)] at 150 °C. Reprinted by permission from Springer[5] and Wiley[6]. Copyrights (2016 and 2018, respectively).

REFERENCES

1. E. Narimissa, V. H. Rolón-Garrido and M. H. Wagner, Rheol. Acta **54** (9-10), 779-791 (2015).
2. E. Narimissa, V. H. Rolón-Garrido and M. H. Wagner, Rheol. Acta **55** (4), 327-333 (2016).
3. E. Narimissa and M. H. Wagner, J. Rheol. **60** (4), 625-636 (2016).
4. E. Narimissa and M. H. Wagner, Polymer **104**, 204–214 (2016).
5. E. Narimissa and M. H. Wagner, Rheol. Acta **55** (8), 633–639 (2016).
6. E. Narimissa and M. H. Wagner, Polymer Engineering & Science (2018).
7. P. Revenu, J. Guillet and C. Carrot, J. Rheology **37** (6), 1041-1056 (1993).
8. J. Sampers and P. J. R. Leblans, J. Non-Newtonian Fluid Mech. **30** (2–3), 325-342 (1988).
9. M. Gupta, Adv. Polym. Tech. **21** (2), 98-107 (2002).
10. M. Padmanabhan and C. W. Macosko, Rheol. Acta **36** (2), 144-151 (1997).
11. K. H. Soon, E. Harkin-Jones, R. S. Rajeev, G. Menary, T. McNally, P. J. Martin and C. Armstrong, Polym. Inter. **58** (10), 1134-1141 (2009).
12. J. Meissner and J. Hostettler, Rheologica Acta **33** (1), 1-21 (1994).
13. E. Narimissa, R. K. Gupta, N. Kao, D. A. Nguyen and S. N. Bhattacharya, Macromolecular Materials & Engineering **299** (7), 851-868 (2014).
14. J. M. Dealy and R. G. Larson, *Structure and Rheology of Molten Polymers - From Structure to Flow Behavior and Back Again*. (Hanser Publishers, Munich, 2006).
15. M. Doi and S. F. Edwards, *The Theory of Polymer Dynamics*. (Oxford University Press, Oxford, 1986).
16. M. H. Wagner, S. Kheirandish and O. Hassager, J. Rheol. **49** (6), 1317-1327 (2005).
17. G. Ianniruberto and G. Marrucci, J. Non-Newtonian Fluid Mech. **65** (2), 241-246 (1996).
18. P. Hachmann, "Multiaxiale Dehnung von Polymerschmelzen," ETH Zurich, 1996.
19. P. Hachmann and J. Meissner, J. Rheol. **47** (4), 989-1010 (2003).
20. H. Bastian, "Non-linear viscoelasticity of linear and long-chain-branched polymer melts in shear and extensional flows," Universität Stuttgart, 2001.
21. M. Kraft, "Untersuchungen zur scherinduzierten rheologischen Anisotropie von verschiedenen Polyethylen-Schmelzen," Diss. Techn. Wiss. ETH Zürich, 1996.
22. M. H. Wagner, P. Rubio and H. Bastian, J. Rheol. **45** (6), 1387-1412 (2001).